Peculiarities of Alfvén wave propagation along a nonuniform magnetic flux tube

Cite as: Phys. Plasmas **12**, 012905 (2005); https://doi.org/10.1063/1.1833392
Submitted: 04 February 2004 . Accepted: 22 October 2004 . Published Online: 22 December 2004

N. V. Erkaev, V. A. Shaidurov, V. S. Semenov, D. Langmayr, and H. K. Biernat

Peculiarities of Alfvén wave propagation along a nonuniform magnetic flux tube

N. V. Erkaev
Intitute of Computational Modelling, Russian Academy of Sciences, Krasnoyarsk 660036, Russia

V. A. Shaidurov
State University of Krasnoyarsk, Krasnoyarsk 660041, Russia

V. S. Semenov
Institute of Physics, State University, St. Petersburg 198504, Russia

D. Langmayr and H. K. Biernat
Space Research Institute, Austrian Academy of Sciences, Schmiedlstrasse 6, A-8042 Graz, Austria

(Received 4 February 2004; accepted 22 October 2004; published online 22 December 2004)

Within the framework of the assumption of large azimuthal wave numbers, the equations for Alfvén and slow magnetosonic waves are obtained using frozen-in material coordinates. These equations are specified for the case of a nonuniform magnetic field with axial symmetry. Assuming a meridional polarization of the magnetic field and velocity perturbations, the effects of Alfvén wave propagation are analyzed which are related to geometric characteristics of a nonuniform magnetic field: (a) A finite curvature radius of the magnetic field lines and (b) convergence of magnetic field lines. The interaction between the Alfvén and magnetosonic waves is found to be strongly dependent on the curvature radius of the magnetic tube and the local plasma β parameter. The electric field amplitude and the length scale of a wave front are found to increase very strongly in the course of the Alfvén wave propagation along a converging magnetic flux tube. Also studied is a temporal decrease of the wave perturbations which is caused by dissipation at the conducting boundary.
 [DOI: 10.1063/1.1833392]

I. INTRODUCTION

Ideal magnetohydrodynamics (MHD) is a commonly used tool for space plasma modeling. However, in general, the nonsteady three-dimensional MHD equations are rather difficult to solve. A possible way is to use asymptotic expansions with respect to small parameters which allows one to simplify MHD problems and to reduce their dimensionality. The thin magnetic flux tube approximation is an example of such an approach which considers a normalized thickness of a magnetic flux tube as a small parameter (see Refs. 1–5). There exist two different kinds of models based on a thin magnetic tube approximation. The first type of models correspond to magnetic flux tubes with plasma characterized by a relatively small plasma pressure compared to the magnetic pressure. But outside of the tubes, the plasma pressure exceeds the magnetic pressure. Such models are relevant to the region of the solar interior. The second type of models consider magnetic flux tubes with an enhanced internal plasma pressure and decreased magnetic pressure. Outside such a tube, the magnetic pressure is much stronger than the plasma pressure. These models are applicable for magnetic flux loops in the solar corona,[6] and also for disturbed magnetic tubes in the magnetospheres of the Earth and other magnetized planets.

With regard to the Earth's magnetosphere, a fruitful assumption of a large azimuthal wave number was used (see Refs. 7–9) which implies that the longitudinal wave length is much larger than the azimuthal one. In this approach, the fast magnetosonic mode is strongly evanescent, and only a transverse Alfvén wave coupled to slow mode magnetosonic waves can be described. In such a case, the perturbation of the total pressure is zero and thus this assumption is relevant to the thin magnetic tube approximation. In particular, this approach was applied for slow magnetosonic pulses propagating along a dipole magnetic tube in the Jovian magnetosphere (see Refs. 10 and 11).

The behavior of the plasma and the dynamics of the magnetic tube are strongly dependent on the ratio of the background plasma and magnetic field pressures in the tube, which is called the β parameter of the plasma. Other important factors are curvature and convergence of magnetic field lines which can affect MHD wave propagations along the magnetic tube.

In our present work we analyze the propagation of Alfvén waves along a nonstraight magnetic tube and, in particular, we focus attention on the effects related to the plasma β parameter, the curvature radius, and the convergence of magnetic field lines. We also study the dissipation of Alfvén waves which is related to their reflections from the boundary with a finite conductivity. We consider the particular case of the meridional polarization of the wave pulses propagating along the magnetic flux tube. The background plasma is assumed to be in equilibrium state with constant temperature and density.

II. BASIC EQUATIONS AND BOUNDARY CONDITIONS

In the dissipationless approximation, the magnetic field and plasma parameters are determined by the ideal MHD

equations[12] which are commonly used for space plasmas,

$$\rho\frac{\partial \mathbf{V}}{\partial t}+\rho(\mathbf{V}\cdot\nabla)\mathbf{V}+\nabla\Pi-\frac{1}{4\pi}(\mathbf{B}\cdot\nabla)\mathbf{B}=0, \tag{1}$$

$$\Pi=P+B^2/(8\pi), \tag{2}$$

$$\frac{\partial\rho}{\partial t}+\mathrm{div}(\rho\mathbf{V})=0,\quad \frac{\partial}{\partial t}\left(\frac{P}{\rho^\gamma}\right)+(\mathbf{V}\cdot\nabla)\left(\frac{P}{\rho^\gamma}\right)=0, \tag{3}$$

$$\frac{\partial\mathbf{B}}{\partial t}-\mathrm{rot}(\mathbf{V}\times\mathbf{B})=0,\quad \mathrm{div}\,\mathbf{B}=0. \tag{4}$$

Here, ρ, $\mathbf{V}$, P, $\mathbf{B}$ are the mass density, velocity, plasma pressure, and magnetic field, respectively. Quantity Π is the total pressure (the sum of magnetic and plasma pressures) and γ is the polytropic index. The assumption of a large azimuthal wave number implies the transversal length scale of a wave perturbation to be much smaller than the longitudinal length scale with respect to the magnetic field. In this approximation the total pressure can be considered to be constant inside the tube and equal to the total pressure outside the tube.

For computational convenience, we introduce dimensionless parameters

$$\tilde{\mathbf{r}}=\mathbf{r}/r_0,\quad \tilde{t}=tV_a/r_0,\quad \tilde{P}=P/(\rho_0V_a^2),$$

$$\tilde{\rho}=\rho/\rho_0,\quad \tilde{\mathbf{B}}=\mathbf{B}/B_0,\quad \tilde{\mathbf{V}}=\mathbf{V}/V_a, \tag{5}$$

where r_0 is a spatial scale used for the normalization, subscript 0 corresponds to background parameters at some point, V_a is the Alfvén velocity, ρ_0 is the background mass density, and B_0 is the characteristic strength of the undisturbed magnetic field. The background plasma pressure and density are considered to be constant.

In dimensionless units, the momentum equation and the total pressure are

$$\tilde{\rho}\frac{\partial\tilde{\mathbf{V}}}{\partial t}+\tilde{\rho}(\tilde{\mathbf{V}}\cdot\nabla)\tilde{\mathbf{V}}+\nabla\tilde{\Pi}-(\tilde{\mathbf{B}}\cdot\nabla)\tilde{\mathbf{B}}=0, \tag{6}$$

$$\tilde{\Pi}=\tilde{P}+\tilde{B}^2/2. \tag{7}$$

In these normalized units, Eqs. (3) and (4) are not changed and thus are the same.

The magnetic field lines are assumed to be connected with a surface which has a finite conductivity. In case of the magnetic tubes in a planetary magnetosphere, a conducting surface is the ionosphere of the planet. At the boundary surface, we use the relationship between the electric field and magnetic field perturbations

$$\frac{c}{4\pi}\mathbf{n}\times\delta\mathbf{B}=\Sigma_s\mathbf{E}, \tag{8}$$

which is based on a local Ohm's law. Here Σ_s is a conductivity of the boundary surface and $\mathbf{n}$ is the normal unit vector. The undisturbed magnetic vector is assumed to be parallel to the unit vector $\mathbf{n}$. For an ideal conducting plasma, the electric field is equal to

$$\mathbf{E}=-\frac{1}{c}\mathbf{V}\times\mathbf{B}, \tag{9}$$

where c is the speed of light and $\mathbf{V}$ is the plasma velocity.

For small perpendicular perturbations, Eqs. (8) and (9) yield

$$\mathbf{V}=\frac{c^2}{4\pi\Sigma_sB}\delta\mathbf{B}. \tag{10}$$

In dimensionless form, Eq. (10) is

$$\tilde{\mathbf{v}}=\frac{\Sigma_a}{\Sigma_s}\delta\tilde{\mathbf{B}}, \tag{11}$$

where Σ_a is the Alfvén conductivity

$$\Sigma_a=\frac{c^2}{4\pi V_{as}} \tag{12}$$

and V_{as} is the local Alfvén speed. This boundary condition determines reflections of incoming MHD waves.

In the following, for simplicity, the tilde for the dimensionless quantities is left out.

III. EQUATIONS FOR A MAGNETIC TUBE IN FROZEN-IN COORDINATES

We introduce frozen-in material coordinates (α,ϕ,ψ) corresponding to Lagrange fluid particles connected with the frozen-in magnetic field lines (see details in the Appendix). The first coordinate α describes the distribution of the mass of plasma along a magnetic flux tube of unit flux, and thus it is expressed by the integral

$$\alpha=\int_0^s\rho/B\,ds', \tag{13}$$

where s is the distance along the magnetic tube. The two other coordinates (ϕ,ψ) are considered to be the Euler potentials for the magnetic field which are defined by the following vector equation:

$$\mathbf{B}=\nabla\phi\times\nabla\psi. \tag{14}$$

From this definition it follows that the gradients of these quantities are orthogonal to the magnetic field:

$$\mathbf{B}\cdot\nabla\phi=0,\quad \mathbf{B}\cdot\nabla\psi=0. \tag{15}$$

This means that the Euler potentials conserve their values along a magnetic field line.

In the frozen-in material coordinates described above and also in the Appendix, we have the system of equations as follows:

$$\frac{\partial\mathbf{V}}{\partial t}-\frac{\partial\mathbf{B}}{\partial\alpha}+\frac{1}{\rho}\nabla\Pi=0, \tag{16}$$

$$P+\frac{1}{2}\mathbf{B}^2=\Pi,\quad \frac{\partial}{\partial t}\left(\frac{\mathbf{B}}{\rho}\right)-\frac{\partial\mathbf{V}}{\partial\alpha}=0, \tag{17}$$

$$\frac{\partial}{\partial t}\left(\frac{P}{\rho^{\gamma}}\right)=0, \quad \frac{D(x,y,z)}{D(\alpha,\phi,\psi)}=\frac{1}{\rho}. \tag{18}$$

Here, $D(x,y,z)/D(\alpha,\phi,\psi)$ is the Jacobian:

$$D(x,y,z)/D(\alpha,\phi,\psi)=x_{\alpha}(y_{\phi}z_{\psi}-y_{\psi}z_{\phi})-x_{\phi}(y_{\alpha}z_{\psi}-y_{\psi}z_{\alpha}) + x_{\psi}(y_{\alpha}z_{\phi}-y_{\phi}z_{\alpha}),$$

where the subscripts (α,ϕ,ψ) denote partial derivatives with respect to the corresponding variables.

The components of velocity and magnetic field are proportional to the corresponding derivatives of the position vector,

$$\mathbf{V}=\frac{\partial \mathbf{r}}{\partial t}, \quad \mathbf{B}=\rho\frac{\partial \mathbf{r}}{\partial \alpha}. \tag{19}$$

Relation (16) is the momentum equation, (17) are the expressions for the total pressure Π and the induction equation, and (18) expresses the adiabatic law and the mass conservation.

IV. DESCRIPTION BY VARIABLES ADAPTED TO A MAGNETIC FLUX TUBE

Hereafter, the magnetic field is assumed to be axisymmetric. Perturbations of a magnetic flux tube can be described in terms of suitable orthogonal curvilinear coordinates σ,λ,ζ related to a given magnetic tube. Here variable σ is considered to characterize the displacement of a fluid particle along a magnetic field line and variables λ,ζ correspond to independent displacements perpendicular with respect to the magnetic field. The total displacement squared is determined by the quadratic form

$$ds^2=g_1d\lambda^2+g_2d\sigma^2+g_3d\zeta^2, \tag{20}$$

where g_1, g_1, and g_3 are the metric coefficients which are expressed through the position vector derivatives with respect to the variables (λ,σ,ζ),

$$g_1=\left|\frac{\partial \mathbf{r}}{\partial \lambda}\right|^2, \quad g_2=\left|\frac{\partial \mathbf{r}}{\partial \sigma}\right|^2, \quad g_3=\left|\frac{\partial \mathbf{r}}{\partial \zeta}\right|^2. \tag{21}$$

The magnetic field strength and velocity squared are determined by the derivatives of the total displacement (20),

$$V^2=g_1\lambda_t^2+g_2\sigma_t^2+g_3\zeta_t^2, \tag{22}$$

$$B^2=\rho^2(g_1\lambda_{\alpha}^2+g_2\sigma_{\alpha}^2+g_3\zeta_{\alpha}^2). \tag{23}$$

Here subscripts "t" and "α" denote derivatives with respect to the time t and mass coordinate α, respectively.

For simplicity, we consider only the case where the metric coefficients as well as the total pressure are not dependent on the parameter ζ.

Finally, transformations to the new variables yield the equations for the parallel and perpendicular displacements,

$$\frac{\partial \sigma_t}{\partial t}-\frac{\partial \rho\sigma_{\alpha}}{\partial \alpha}+\frac{1}{g_2}\frac{\partial g_2}{\partial \lambda}(\sigma_t\lambda_t-\rho\sigma_{\alpha}\lambda_{\alpha})+\frac{1}{2g_2}\frac{\partial g_2}{\partial \sigma}(\sigma_t^2-\rho\sigma_{\alpha}^2) - \frac{1}{2g_2}\frac{\partial g_1}{\partial \sigma}(\lambda_t^2-\rho\lambda_{\alpha}^2)-\frac{1}{2g_2}\frac{\partial g_3}{\partial \sigma}(\zeta_t^2-\rho\zeta_{\alpha}^2)+\frac{1}{\rho g_2}\frac{\partial \Pi}{\partial \sigma}=0, \tag{24}$$

$$\frac{\partial \lambda_t}{\partial t}-\frac{\partial \rho\lambda_{\alpha}}{\partial \alpha}+\frac{1}{g_1}\frac{\partial g_1}{\partial \sigma}(\sigma_t\lambda_t-\rho\sigma_{\alpha}\lambda_{\alpha})+\frac{1}{2g_1}\frac{\partial g_1}{\partial \lambda}(\lambda_t^2-\rho\lambda_{\alpha}^2) - \frac{1}{2g_1}\frac{\partial g_2}{\partial \lambda}(\sigma_t^2-\rho\sigma_{\alpha}^2)-\frac{1}{2g_1}\frac{\partial g_3}{\partial \lambda}(\zeta_t^2-\rho\zeta_{\alpha}^2)+\frac{1}{\rho g_1}\frac{\partial \Pi}{\partial \lambda}=0, \tag{25}$$

$$\frac{\partial \zeta_t}{\partial t}-\frac{\partial \rho\zeta_{\alpha}}{\partial \alpha}+\frac{1}{g_3}\frac{\partial g_3}{\partial \lambda}(\zeta_t\lambda_t-\rho\zeta_{\alpha}\lambda_{\alpha}) + \frac{1}{g_3}\frac{\partial g_3}{\partial \sigma}(\zeta_t\sigma_t-\rho\zeta_{\alpha}\sigma_{\alpha})+\frac{1}{\rho g_3}\frac{\partial \Pi}{\partial \zeta}=0. \tag{26}$$

This system of coupled partial differential equations describes the propagation of transverse and field-aligned MHD waves along a curved thin magnetic flux tube. These equations allow one to analyze the effects of interaction between the transverse and field-aligned modes, as well as the effects related to the convergence of the magnetic field lines.

The field-aligned equation is transformed into

$$\frac{\partial(\sqrt{g_2}\sigma_t)}{\partial t}-\frac{\partial(\sqrt{g_2}\rho\sigma_{\alpha})}{\partial \alpha}+\frac{1}{2\sqrt{g_2}}\frac{\partial g_2}{\partial \lambda}(\sigma_t\lambda_t-\rho\sigma_{\alpha}\lambda_{\alpha}) - \frac{1}{2\sqrt{g_2}}\frac{\partial g_1}{\partial \sigma}(\lambda_t^2-\rho\lambda_{\alpha}^2)-\frac{1}{2\sqrt{g_2}}\frac{\partial g_3}{\partial \sigma}(\zeta_t^2-\rho\zeta_{\alpha}^2)+\frac{1}{\rho\sqrt{g_2}}\frac{\partial \Pi}{\partial \sigma}=0. \tag{27}$$

The total pressure derivative is

$$\frac{\partial \Pi}{\partial \sigma}=\frac{\partial \Pi}{\partial \alpha}\frac{1}{\sigma_{\alpha}}-\left(\frac{\partial \Pi}{\partial \lambda}\lambda_{\alpha}+\frac{\partial \Pi}{\partial \zeta}\zeta_{\alpha}\right)\frac{1}{\sigma_{\alpha}}. \tag{28}$$

Hereafter, we assume the total pressure to be a function of two variables λ, σ and thus we cancel the derivative $\partial\Pi/\partial\zeta$ in the further expressions. The total pressure definition leads to the equation

$$\frac{1}{\sqrt{g_2}\rho\sigma_{\alpha}}\frac{\partial \Pi}{\partial \alpha}-\frac{\partial(\rho\sqrt{g_2}\sigma_{\alpha})}{\partial \alpha} = \frac{\partial P}{\partial \alpha}\frac{1}{\sqrt{g_2}\rho\sigma_{\alpha}}+\frac{1}{\sqrt{g_2}\rho\sigma_{\alpha}}\frac{\partial}{\partial \alpha}(g_1\rho^2\lambda_{\alpha}^2+g_3\rho^2\zeta_{\alpha}^2). \tag{29}$$

Using Eqs. (28) and (29), we transform Eq. (27) to

$$\frac{\partial(\rho\sqrt{g_2}\sigma_t)}{\partial t}+\frac{1}{\rho\sqrt{g_2}\sigma_{\alpha}}\frac{\partial P}{\partial \alpha}+\frac{1}{2\sqrt{g_2}}\frac{\partial g_2}{\partial \lambda}(\sigma_t\lambda_t)-\frac{1}{2\sqrt{g_2}} \times\frac{\partial g_1}{\partial \sigma}(\lambda_t^2-\rho\lambda_{\alpha}^2)-\frac{1}{2\sqrt{g_2}}\frac{\partial g_3}{\partial \sigma}(\zeta_t^2-\rho\zeta_{\alpha}^2)+\frac{1}{\sqrt{g_2}\rho\sigma_{\alpha}}\frac{\partial}{\partial \alpha} \times(g_1\rho^2\lambda_{\alpha}^2+g_3\rho^2\zeta_{\alpha}^2)-\frac{1}{\rho\sqrt{g_2}\sigma_{\alpha}}\left(\frac{\partial \Pi}{\partial \lambda}+\frac{1}{2}\frac{\partial g_2}{\partial \lambda}\rho^2\sigma_{\alpha}^2\right)\lambda_{\alpha} =0, \tag{30}$$

where the plasma pressure P and the density ρ are coupled by the adiabatic equation

$$P=\tfrac{1}{2}\beta_0\rho^{\gamma}, \tag{31}$$

and the density is determined by the algebraic equation

$$\tfrac{1}{2}\beta_0\rho^\gamma + \tfrac{1}{2}g_1\rho^2\lambda_\alpha^2 + \tfrac{1}{2}g_2\rho^2\sigma_\alpha^2 + \tfrac{1}{2}g_3\rho^2\zeta_\alpha^2 = \Pi(\lambda,\sigma,\zeta). \quad (32)$$

Here, quantity β_0 is the plasma β parameter defined as $\beta_0 = 8\pi P_0/B_0^2$, where P_0 and B_0 are the dimensional values of the plasma pressure and the magnetic field strength used for the normalization (5).

Next we transform Eq. (25) for the transverse component λ. Assuming the background plasma to be in a hydrostatic equilibrium, we have a relation between the magnetic tension and the total pressure gradient

$$\frac{\partial\Pi}{\partial\lambda} + \frac{1}{2q_2}\frac{\partial g_2}{\partial\lambda}B^2 = 0. \quad (33)$$

Here, B is the background magnetic field strength which is assumed to be a known function of λ, σ.

Using the latter equation, we substitute the expression for the total pressure gradient into Eq. (25)

$$\frac{\partial\lambda_t}{\partial t} - \frac{\partial\rho\lambda_\alpha}{\partial\alpha} + \frac{1}{g_1}\frac{\partial g_1}{\partial\sigma}(\sigma_t\lambda_t - \rho\sigma_\alpha\lambda_\alpha) + \frac{1}{2g_1}\frac{\partial g_1}{\partial\lambda}(\lambda_t^2 - \rho\lambda_\alpha^2) - \frac{1}{2g_1}\frac{\partial g_2}{\partial\lambda}\sigma_t^2 + \frac{1}{2g_1g_2\rho}\frac{\partial g_2}{\partial\lambda}(g_2\rho^2\sigma_\alpha^2 - B^2) - \frac{1}{2g_1}\frac{\partial g_3}{\partial\lambda}(\zeta_t^2 - \rho\zeta_\alpha^2) = 0. \quad (34)$$

The total pressure can be expressed through the background parameters

$$\Pi = \tfrac{1}{2}\beta_0 + \tfrac{1}{2}B^2. \quad (35)$$

From Eqs. (32) and (35) for the total pressure, it follows that

$$g_2\rho^2\sigma_\alpha^2 - B^2 = \beta_0(1-\rho^\gamma) - g_1\rho^2\lambda_\alpha^2 - g_3\rho^2\zeta_\alpha^2. \quad (36)$$

Taking into account Eq. (36), we finally obtain

$$\frac{\partial(\sqrt{g_2}\sigma_t)}{\partial t} + \frac{1}{\rho\sqrt{g_2}\sigma_\alpha}\frac{\partial P}{\partial\alpha} + \frac{1}{2\sqrt{g_2}}\frac{\partial g_2}{\partial\lambda}(\sigma_t\lambda_t) - \frac{1}{2\sqrt{g_2}}\frac{\partial g_1}{\partial\sigma}(\lambda_t^2 - \rho\lambda_\alpha^2) - \frac{1}{2\sqrt{g_2}}\frac{\partial g_3}{\partial\sigma}(\zeta_t^2 - \rho\zeta_\alpha^2) + \frac{1}{\sqrt{g_2}\rho\sigma_\alpha}\frac{\partial}{\partial\alpha}(g_1\rho^2\lambda_\alpha^2 + g_3\rho^2\zeta_\alpha^2) - \frac{1}{\rho\sqrt{g_2}\sigma_\alpha}\frac{1}{2g_2}\frac{\partial g_2}{\partial\lambda}[\beta_0(1-\rho^\gamma) - g_1\rho^2\lambda_\alpha^2 - g_3\rho^2\zeta_\alpha^2]\lambda_\alpha = 0,$$

$$\frac{\partial\lambda_t}{\partial t} - \frac{\partial\rho\lambda_\alpha}{\partial\alpha} + \frac{1}{g_1}\frac{\partial g_1}{\partial\sigma}(\sigma_t\lambda_t - \rho\sigma_\alpha\lambda_\alpha) + \frac{1}{2g_1}\frac{\partial g_1}{\partial\lambda}(\lambda_t^2 - \rho\lambda_\alpha^2) - \frac{1}{2g_1}\frac{\partial g_2}{\partial\lambda}\sigma_t^2 + \frac{1}{2g_1g_2\rho}\frac{\partial g_2}{\partial\lambda}[\beta_0(1-\rho^\gamma) - g_1\rho^2\lambda_\alpha^2 - g_3\rho^2\zeta_\alpha^2] - \frac{1}{2g_1}\frac{\partial g_3}{\partial\lambda}(\zeta_t^2 - \rho\zeta_\alpha^2) = 0. \quad (37)$$

This system of equations can substantially be simplified after neglecting the second order terms with respect to the perturbations. Thus, the linearized equations are

$$\frac{\partial(\sqrt{g_2}\sigma_t)}{\partial t} + \frac{1}{B}\frac{\partial\delta P}{\partial\alpha} = 0, \quad (38)$$

$$\frac{\partial(g_1\lambda_t)}{\partial t} - \frac{\partial(g_1\lambda_\alpha)}{\partial\alpha} - \frac{1}{g_2\rho}\frac{\partial g_2}{\partial\lambda}\delta P = 0, \quad (39)$$

$$\frac{\partial(g_3\zeta_t)}{\partial t} - \frac{\partial(g_3\zeta_\alpha)}{\partial\alpha} = 0, \quad (40)$$

where

$$\delta P = \frac{\gamma\beta_0}{\beta_0(\gamma-2) + 4\Pi}\left[\left(\frac{\partial\Pi}{\partial\sigma} - \frac{\partial g_2}{\partial\sigma}\frac{B^2}{2g_2}\right)\delta\sigma + \left(\frac{\partial\Pi}{\partial\lambda} - \frac{\partial g_2}{\partial\lambda}\frac{B^2}{2g_2}\right)\delta\lambda - \sqrt{g_2}B\delta\sigma_\alpha\right]. \quad (41)$$

The background dimensionless density is assumed to be constant, $\rho = 1$.

One can see that Eq. (39) for the perpendicular perturbation $\delta\lambda$ is coupled with the plasma pressure perturbation by the term proportional to the plasma β parameter β_0. And the equation for the field-aligned perturbations is coupled with the perpendicular perturbations by the term in expression (41) which is also proportional to the plasma β parameter.

V. EFFECTS OF A CURVATURE OF MAGNETIC FIELD LINES

To analyze the effects related to a finite curvature of magnetic field lines, we consider a simple magnetic field configuration with azimuthal magnetic field. The geometrical situation for this case is shown in Fig. 1(a).

In such a case, appropriate coordinates are the cylindrical ones (r,θ,z). In the equations above, we substitute cylindrical coordinates and the corresponding metric coefficients, instead of the general ones, which are given by

$$\lambda = r, \quad \sigma = \theta, \quad \zeta = z, \quad g_1 = 1, \quad g_2 = r^2, \quad g_3 = 1. \quad (42)$$

Then, the system of equations [Eqs. (38)–(41)] is reduced to

$$\frac{\partial(r\delta\theta_t)}{\partial t} + \frac{1}{B}\frac{\partial\delta P}{\partial\alpha} = 0, \quad (43)$$

$$\frac{\partial\delta r_t}{\partial t} - \frac{\partial\delta r_\alpha}{\partial\alpha} - \frac{2}{r}\delta P = 0, \quad (44)$$

$$\frac{\partial\delta z_t}{\partial t} - \frac{\partial\delta z_\alpha}{\partial\alpha} = 0, \quad (45)$$

where

$$\delta P = \frac{\gamma\beta_0}{\beta_0(\gamma-2) + 4\Pi}\left[\left(\frac{\partial\Pi}{\partial r} - \frac{B^2}{r}\right)\delta r - rB\delta\theta_\alpha\right]. \quad (46)$$

The undisturbed magnetic field lines are circles, and thus the background magnetic field strength and radius are constant along the magnetic tube. The normalized values are

$$B = 1, \quad r = 1. \quad (47)$$

The total pressure is a function of r. In our normalized units it is $\Pi = 1/(2r^2) + \beta_0/2$, and thus the gradient of the total pressure is

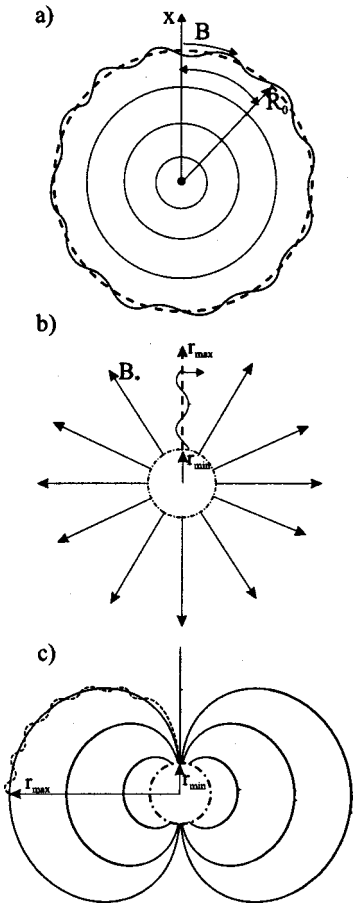

FIG. 1. Sketches of a magnetic field geometry for three models: (a) Azimuthal magnetic field, (b) radial magnetic field, and (c) dipole magnetic field.

$$\frac{\partial \Pi}{\partial r} = -\frac{1}{r^3} = -1. \tag{48}$$

Substituting expression (46) for the plasma pressure perturbation, we obtain the equations

$$\frac{\partial \delta\theta_t}{\partial t} - \epsilon \frac{\partial \delta\theta_\alpha}{\partial \alpha} - 2\epsilon \delta r_\alpha = 0, \tag{49}$$

$$\frac{\partial \delta r_t}{\partial t} - \frac{\partial \delta r_\alpha}{\partial \alpha} + 2\epsilon \delta\theta_\alpha + 4\epsilon \delta r = 0, \tag{50}$$

$$\frac{\partial \delta z_t}{\partial t} - \frac{\partial \delta z_\alpha}{\partial \alpha} = 0,$$

where

$$\epsilon = \frac{\gamma\beta_0}{2 + \gamma\beta_0}. \tag{51}$$

One can see from Eqs. (49) and (50) that the interaction between transverse and field-aligned wave perturbations is controlled by the plasma β parameter.

It is useful to rewrite system [Eqs. (49) and (50)] in dimensional form with respect to the longitudinal $\delta s = R\delta\theta$ and perpendicular δr displacements

$$\frac{\partial^2 \delta s}{\partial t^2} - \epsilon V_a^2 \frac{\partial^2 \delta s}{\partial s^2} - 2\epsilon V_a^2 \frac{1}{R}\frac{\partial \delta r}{\partial s} = 0, \tag{52}$$

$$\frac{\partial^2 \delta r}{\partial t^2} - V_a^2 \frac{\partial^2 \delta r}{\partial s^2} + 2\epsilon V_a^2 \frac{1}{R}\frac{\partial \delta s}{\partial s} + 4\epsilon V_a^2 \frac{1}{R^2}\delta r = 0, \tag{53}$$

$$\frac{\partial^2 \delta z}{\partial t^2} - V_a^2 \frac{\partial^2 \delta z}{\partial s^2} = 0. \tag{54}$$

Here s is the distance along the magnetic field line, V_a is the Alfvén speed, and R is the curvature radius of the magnetic field line. The equations for the transverse δr and longitudinal δs modes are coupled by the terms proportional to $\beta_0 V_a^2/R$. The third equation for the perturbations along the z axis is not coupled with the others.

Fourier transformations applied to Eqs. (52) and (53) lead to the algebraic system for the amplitudes

$$(\epsilon V_a^2 k^2 - \omega^2)\delta s + 2ik\epsilon V_a^2 \frac{1}{R}\delta r = 0, \tag{55}$$

$$-2ik\epsilon V_a^2 \frac{1}{R}\delta s + \left(V_a^2 k^2 - \omega^2 + 4\epsilon V_a^2 \frac{1}{R^2}\right)\delta r = 0. \tag{56}$$

The dispersion equation is given by

$$\omega^4 - \omega^2[(kV_a)^2(\epsilon + 1) + 4\epsilon V_a^2/R^2] + \epsilon(kV_a)^4 = 0. \tag{57}$$

The dispersion equation determines two phase velocities corresponding to the fast (V_f) and the slow (V_s) modes,

$$V_f = V_a\{(\epsilon + 1)/2 + 2\epsilon/(kR)^2 + \sqrt{(1-\epsilon)^2/4 + 2\epsilon(\epsilon+1)/(kR)^2 + 4\epsilon^2/(kR)^4}\}^{1/2}, \tag{58}$$

$$V_s = V_a\sqrt{\epsilon}/\{(\epsilon + 1)/2 + 2\epsilon/(kR)^2 + \sqrt{(1-\epsilon)^2/4 + 2\epsilon(\epsilon+1)/(kR)^2 + 4\epsilon^2/(kR)^4}\}^{1/2}. \tag{59}$$

In the particular case of a straight magnetic tube the transverse and longitudinal modes are completely decoupled. In the limiting case $R \to \infty$, expressions (58) and (59) are simplified to those corresponding to the fast and slow phase velocities for a straight magnetic tube:

$$V_f = V_a = \frac{B_0}{\sqrt{4\pi\rho_0}}, \tag{60}$$

$$V_s = \sqrt{\epsilon}V_a = \frac{\sqrt{\gamma P_0}B_0}{\sqrt{\gamma P_0 4\pi + B_0^2}} = \frac{C_s V_a}{\sqrt{C_s^2 + V_a^2}}. \tag{61}$$

Here C_s is the sonic speed. In our study, the background plasma parameters inside the magnetic tube are considered to be equal to the external ones. In this particular case the phase speed of the fast kink mode is equal to the Alfvén speed. In the more general case of different internal and external parameters, the phase speed of a fast kink is between the external and internal Alfvén speeds.[6,13] In the approximation of a large azimuthal wave number (the longitudinal wave length

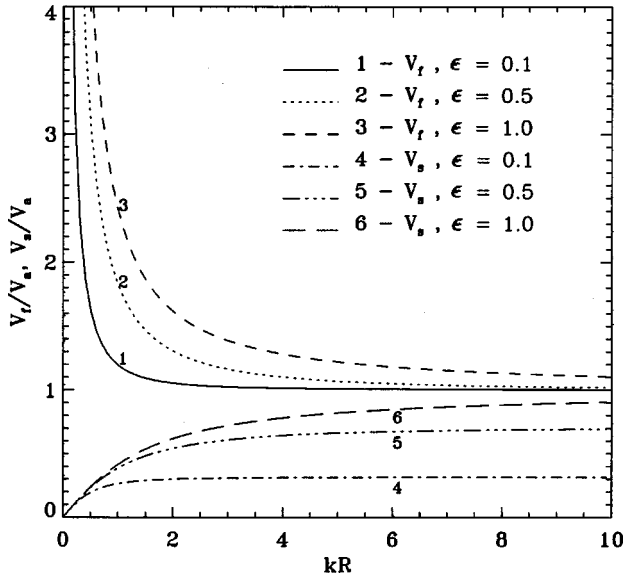

FIG. 2. Phase velocities of the Alfvén (curves 1, 2, and 3) and slow magnetosonic (curves 4, 5, and 6) waves corresponding to ϵ parameters (1, 0.5, 0.1), respectively.

is much larger than the perpendicular one), the phase speed of the slow magnetosonic wave (sausage mode) is determined by the internal magnetic field and plasma parameters.

For a finite kR, the phase velocity is a function of the wave number. For large numbers $kR \gg 1$, the asymptotic expressions in terms of order $1/(kR)$ are given by

$$V_f \approx V_a\left[1 + 2\frac{\epsilon}{(1-\epsilon)}\frac{1}{(kR)^2}\right] = V_a[1 + \gamma\beta_0/(kR)^2], \quad (62)$$

$$V_s \approx \frac{V_a C_a}{\sqrt{V_a^2 + C_s^2}}\left[1 + 2\frac{\epsilon}{(1-\epsilon)}\frac{1}{(kR)^2}\right]^{-1} = \frac{V_a C_s}{\sqrt{V_a^2 + C_s^2}}\frac{1}{[1 + \gamma\beta_0/(kR)^2]}. \quad (63)$$

Here terms of order $1/(kR)^4$ are neglected. These formulas show the dispersion effects to be of order $\beta/(kR)^2$.

From Eqs. (55) and (56) we find a relationship between the transverse and field-aligned perturbations. For the fast kink mode, the field-aligned displacement and velocity induced by the transverse perturbation are given by

$$\delta s = 2ikV_a^2\frac{\epsilon}{R}\frac{\delta r}{(\omega^2 - \epsilon V_a^2 k^2)} \approx 2i\frac{\epsilon}{kR}\frac{\delta r}{(1-\epsilon)}, \quad (64)$$

$$\delta v_s = i\omega\delta s \approx -2V_a\frac{\epsilon}{R}\frac{\delta r}{(1-\epsilon)}. \quad (65)$$

The last two equations contain only the first order terms with respect to the curvature $(\sim 1/R)$.

The phase velocities given by formulas (58) and (59) are shown in Fig. 2 as functions of the dimensionless parameter kR. Curves 1, 2, and 3 are corresponding to the Alfvén wave for ϵ's 0.1, 0.5, 1, and curves 4, 5, and 6 are corresponding to the magnetosonic slow wave for the same ϵ.

In a curved magnetic tube, the phase velocity of the Alfvén wave is larger than that in a straight magnetic tube. With regard to the slow mode waves propagating along a curved magnetic tube, the curvature effect is quite opposite. The phase velocity of a slow magnetosonic wave in a curved magnetic tube is less than that in a straight tube.

This effect can be explained qualitatively as follows: If a curved magnetic tube is pushed radially away or towards the center of curvature, then the variation of the volume of the magnetic tube leads to a decrease or increase of the plasma density and pressure, respectively. The variation of the plasma pressure is proportional to the displacement $\delta\lambda$, namely, $\delta P \propto -\delta\lambda\beta_0/R$. In a curved magnetic field, the magnetic tension leads to a force of buoyancy affecting the magnetic flux tube. In particular, this buoyancy is the reason for interchange instability. Magnetic tubes with enhanced plasma pressure are forced to move away from the center of curvature. In the opposite case of a decreased plasma pressure inside the tube, the buoyancy force is directed towards the curvature center. Hence the magnetic field curvature causes the additional buoyancy force $(f \propto -\delta P/R \propto \delta\lambda\beta_0/R^2)$ which is acting opposite to the displacement of the magnetic field line. This force is the reason for the dispersion effect. Because of this force, the resulting rigidity of the curved magnetic field line is larger and the oscillation period T is shorter than that of a straight magnetic tube for the same wave length. Therefore, in a curved magnetic tube, the phase velocity of the fast kink mode is larger than that in a straight magnetic tube for the same wave length.

In the case of a slow magnetosonic wave, the plasma pressure perturbations are propagating along the magnetic tube. For positive and negative plasma pressure perturbations, the buoyancy force is directed outwards and towards the curvature center, respectively. The resulting buoyancy force acting on a small part of the magnetic tube has a nonzero projection along the curved magnetic field line, and it compensates partially for the force of the plasma pressure gradient. This effect is diminishing the resulting force acting opposite to the longitudinal displacement. Because of that the period of the slow wave oscillation is larger, and the slow wave speed is less than that in a straight magnetic tube for the same wave number.

Figures 3 and 4 present the results of calculations of a pulse propagation for the initial perpendicular displacement and plasma velocity,

$$\delta r = \delta r_0 \exp(-20\alpha^2), \quad \theta = \alpha,$$

$$\delta r_t = -40\,\delta r_0 \alpha \exp(-20\alpha^2). \quad (66)$$

The initial field-aligned perturbations are assumed to be zero.

The calculation results correspond to a plasma β, $\beta_0 = 0.1$, and a polytropic index, $\gamma = 2$. The numerical solution is obtained on the base of a finite difference Lax–Wendroff scheme.

Figure 3 shows the radial displacement and the radial components of the magnetic field and velocity as functions of the azimuthal angle for different times.

In addition, Fig. 4 shows the azimuthal displacement and azimuthal components of the magnetic field and velocity as

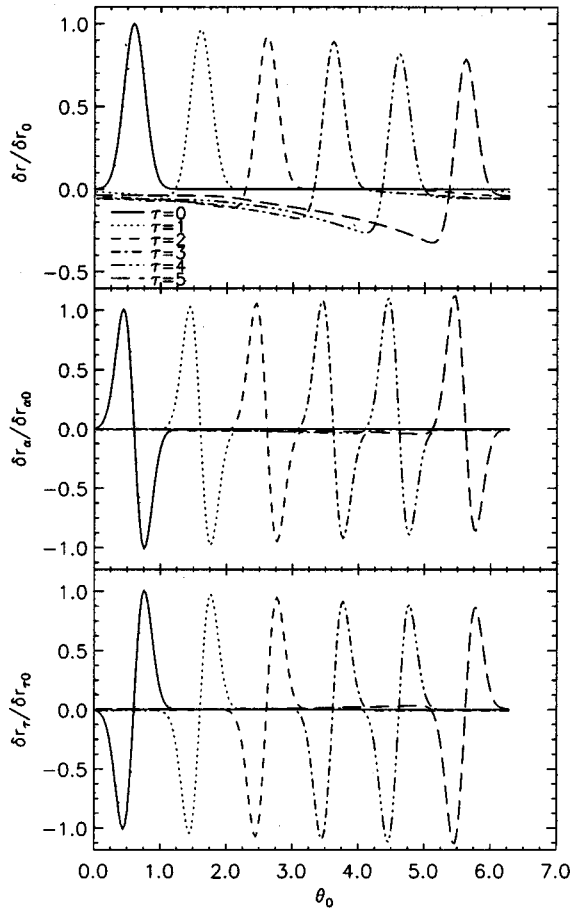

FIG. 3. Transverse displacement and perturbations of the magnetic field and velocity corresponding to the Alfvén pulse in the azimuthal tube.

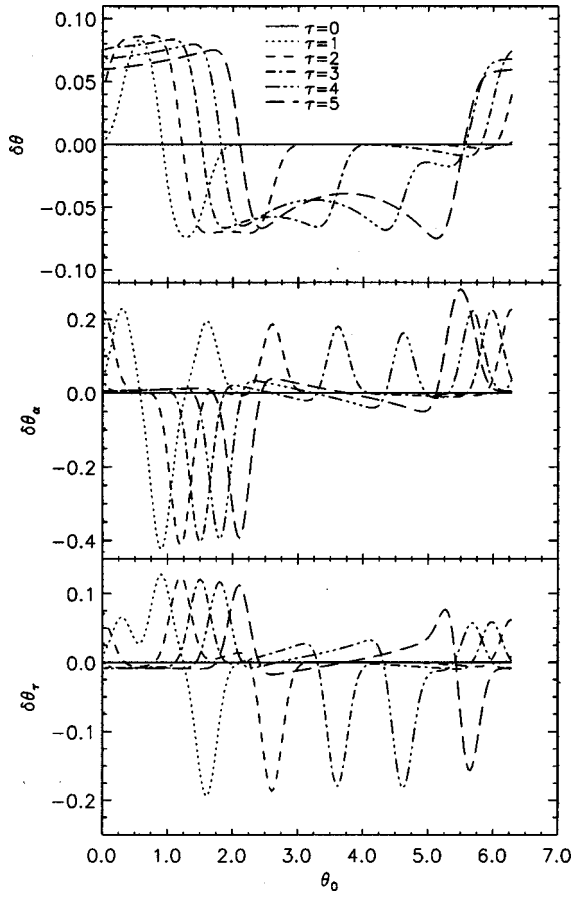

FIG. 4. Longitudinal displacement and field-aligned perturbations of the magnetic field and velocity induced by the Alfvén pulse in the azimuthal magnetic tube.

functions of the azimuthal angle for different times. The perturbations are scaled to the initial radial displacement amplitude δr_0.

As can be seen in the figures, the perpendicular perturbations induce the field-aligned compressible perturbations which are of two types. The first one is a slow magnetosonic wave propagating with sonic speed along the magnetic tube. The second one is a compressible mode propagating together with the perpendicular perturbations with Alfvén speed. These results indicate that in a curved magnetic flux tube, Alfvén waves are not incompressible. They are accompanied by perturbations of the plasma pressure and density, as well as a field-aligned velocity. The amplitude of the field-aligned plasma velocity perturbation is approximately proportional to the background plasma β parameter. The dimensional parallel velocity amplitude is about $2\beta_0 V_a \delta r/R$.

In addition, the curvature of magnetic field lines brings about dispersion effects for Alfvén waves which are related to the last term in Eq. (50).

VI. ALFVÉN WAVES IN A CONVERGING MAGNETIC FIELD

In this section, we study an influence of convergence of magnetic field lines on Alfvén wave propagation along a magnetic flux tube. We first consider a simple model of the magnetic field configuration with straight magnetic field lines perpendicular to a Z axis, which are converging radially towards this axis. The geometrical situation corresponding to this model is shown in Fig. 1(b). In this case we also use cylindrical coordinates (r,θ,z). In Eqs. (38)–(40) we substitute the cylindrical coordinates and the specified metric coefficients,

$$\lambda=\theta, \quad \sigma=r, \quad \zeta=z, \quad g_1=r^2, \quad g_2=1, \quad g_3=1. \tag{67}$$

After substituting the metric coefficients, the system of equations (38), (34), and (40) yields

$$\frac{\partial(r^2\delta\theta_t)}{\partial t}-\frac{\partial(r^2\delta\theta_\alpha)}{\partial\alpha}=0, \tag{68}$$

$$\frac{\partial\delta r_t}{\partial t}+\frac{1}{B}\frac{\partial\delta P}{\partial\alpha}=0, \tag{69}$$

$$\delta P=-\frac{\gamma\beta_0 r^2}{(2+\gamma\beta_0 r^2)}\left(\frac{\delta r}{r^3}+\frac{\delta r_\alpha}{r}\right), \tag{70}$$

$$\frac{\partial\delta z_t}{\partial t}-\frac{\partial\delta z_\alpha}{\partial\alpha}=0, \tag{71}$$

where $r=\sqrt{2\alpha}$

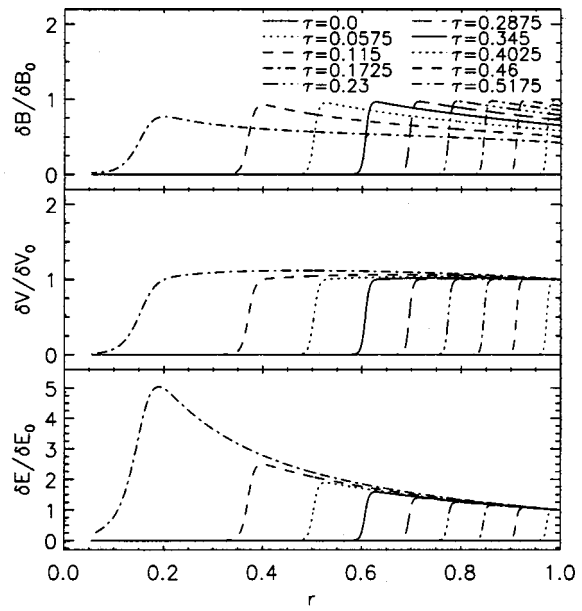

FIG. 5. Propagation of the wave front along the radially converging magnetic field towards the center of the field.

The radial magnetic field lines are not curved, and thus there is no interaction between Alfvén and compressible waves.

Figure 5 shows the propagation of the wave front carrying the electric field along the radial magnetic tube. From top to bottom there are shown the magnetic field, the velocity, and the electric field perturbations, respectively, as functions of the distance for different times. The wave is produced by the plasma acceleration at the magnetic tube boundary ($r=1, \alpha=0.5$), where the velocity is given as an increasing function of time with a saturation

$$\delta\lambda_t = V(t) = \delta V_0\{\tanh[200(t-0.3)]+1\}. \tag{72}$$

The initial displacement and its derivatives are assumed to be equal to zero. The initial plasma β is taken to be $\beta_0=0.1$.

At the conducting boundary ($r_{\min}$) we use condition (10) for the perpendicular perturbations

$$\theta_t - \mu\theta_\alpha = 0, \tag{73}$$

where parameter μ characterizes the dissipative properties of the boundary. The limiting cases $\mu=0$ and $\mu=\infty$ correspond to ideal conducting and dielectric surfaces, respectively.

The length scale of the wave front is increasing in the course of the wave propagation towards the strong magnetic field region. While the wave front does not arrive at the reflection zone, the amplitudes of velocity and magnetic field perturbations do not change much. In the reflection zone, these perturbations decrease substantially towards the boundary. The electric field amplitude has a rather strong enhancement and it reaches its maximum at the conducting boundary.

After each reflection, the wave loses part of its energy. The loss of the wave energy is dependent on the conductivity of the boundary surface as well as on the ratio $r_{\max}/r_{\min}$.

The next model with a strongly converging magnetic field is that of a dipole magnetic field. In this case, the most convenient way to study the effects of the wave propagation is given within the frame of dipole coordinates.[14] The relation between the usually used spherical coordinates (r,θ) and the dipolar coordinates (λ,σ) are given by the field line equation and a function describing the normal to it. These two relations are of the following form:

$$r = \lambda \sin^2\theta, \quad r = \sigma\sqrt{\cos\theta}. \tag{74}$$

The displacement ds is found to be given by

$$ds^2 = r^2 d\theta^2 + dr^2 + r^2 \sin^2\theta d\varphi^2$$
$$= \frac{\sin^6\theta}{1+3\cos^2\theta} d\lambda^2 + \frac{4\cos^3\theta}{1+3\cos^2\theta} d\sigma^2 + r^2\sin^2\theta d\phi^2, \tag{75}$$

where φ is the azimuthal angle. In accordance with Eqs. (74) and (75), the metric coefficients can be expressed through the θ angle

$$g_1 = \frac{\sin^6\theta}{1+3\cos^2\theta}, \tag{76}$$

$$g_2 = \frac{4\cos^3\theta}{1+3\cos^2\theta}, \tag{77}$$

$$g_3 = r^2\sin^2\theta. \tag{78}$$

The spherical radius as a function of σ and λ is implicitly given by the equation

$$\frac{r(\lambda,\sigma)}{\lambda} + \frac{r(\lambda,\sigma)^4}{\sigma^4} = 1. \tag{79}$$

Substituting for θ, we express the metric coefficients through the function $r(\lambda,\sigma)$ as follows:

$$g_1(\lambda,\sigma) = \frac{r(\lambda,\sigma)^3}{\lambda^3}\frac{1}{1+3r(\lambda,\sigma)^4/\sigma^4}, \tag{80}$$

$$g_2(\lambda,\sigma) = 4\frac{r(\lambda,\sigma)^6}{\lambda^6}\frac{1}{1+3r(\lambda,\sigma)^4/\sigma^4}, \tag{81}$$

$$g_3(\lambda,\sigma) = r(\lambda,\sigma)^3/\lambda. \tag{82}$$

For the normalization (5) we use the following parameters:

$$B_0 = B_d(r_{\min}/r_{\max})^3, \quad r_0 = r_{\max}, \quad V_a = B_0/\sqrt{4\pi\rho_0}. \tag{83}$$

Here B_d is the dipole magnetic field strength at the dissipative boundary of the magnetic tube ($r=r_{\min}$).

The initial plasma β is taken to be $\beta_0=0.1$. At the equatorial edge of the tube ($r_{\max}=1$), we use a boundary condition corresponding to a monotonic increase of the plasma velocity with the saturation

$$\delta\lambda_t = V(t) = \delta V_0\{\tanh[200(t-0.009)]+1\}, \quad \alpha = 0.45. \tag{84}$$

The initial displacement as well as the magnetic field perturbation are assumed to vanish. At the conducting surface for $r_{\min}$ we assume condition (11) with the coefficient $\mu=\Sigma_a/\Sigma_s=0.5$.

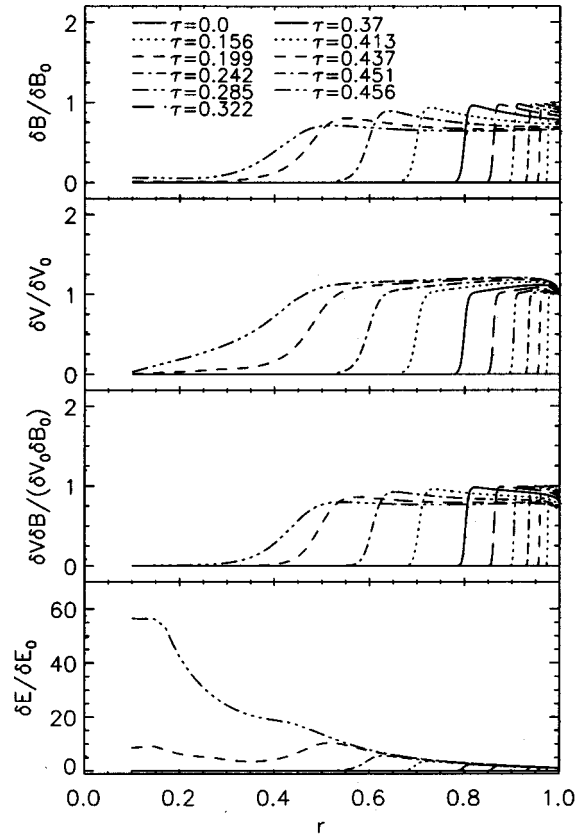

FIG. 6. Propagation of the wave front along the dipole magnetic tube towards the dipole.

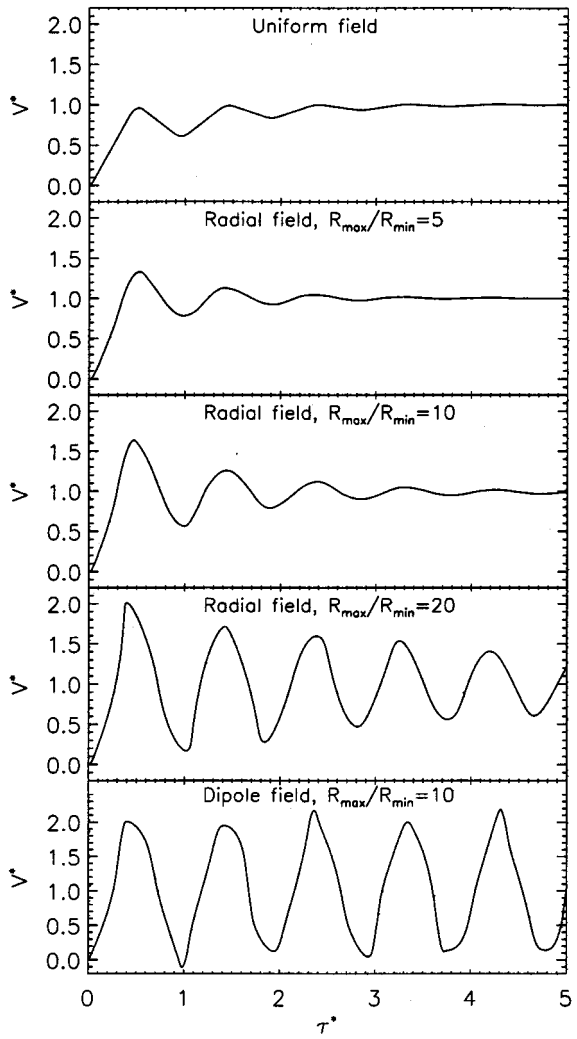

FIG. 7. Average velocity perturbations in the tube as functions of time in the cases of uniform, radial, and dipole magnetic flux tubes.

Figure 6 shows the propagation of the wave front along the dipole magnetic tube. This wave carries the electric field from the equatorial boundary under the condition (84). From top to bottom there are shown the magnetic field, the velocity, and the electric field perturbations, respectively, as functions of the radial distance for different times in units of $r_{\max}/V_a$. The ratio $r_{\max}/r_{\min}$ is assumed to be equal to 10.

Until the reflection zone, the velocity amplitude increases only slightly during the wave propagation. In the reflection zone, the amplitudes of the velocity and the magnetic field perturbations are decreasing functions of the radius r, and they are very small in the vicinity of the conducting boundary $r_{\min}$.

The electric field amplitude is obtained by multiplication of the plasma velocity amplitude with the dipole magnetic field strength, and it gives evidence of a monotonic increase until the conducting boundary.

Figure 7 indicates the influence of the magnetic field convergence on the wave dissipation. We present the average velocity perturbations in the different model magnetic tubes as functions of time. The velocity is normalized to its asymptotic values, and the time is scaled to the double time interval of the Alfvén wave propagation from one boundary to the other. From top to bottom we show the plots corresponding to the different models: A uniform magnetic tube; radial magnetic tubes for three ratios of $r_{\max}/r_{\min}$; a dipole magnetic tube for $r_{\max}/r_{\min}=10$. The dissipative parameter of the conductive surface is the same for all cases, namely, $\mu=0.5$.

In the case of the uniform magnetic tube, convergence effects are absent. For the radial magnetic tube, convergence effects exist and they are stronger for larger ratios of $r_{\max}/r_{\min}$. For the dipole tube, convergence effects are the most pronounced. One can see from the figure that the convergence of the magnetic field brings about an enhancement of the relaxation time for Alfvén waves in the magnetic tube. For the uniform magnetic field, perturbations practically disappear after two reflections. But in the case of the dipole field, the Alfvén waves manifest to have many reflections without a noticeable decrease of their amplitude.

VII. CONCLUSIONS

A large azimuthal wave number approach is applied to MHD waves propagating along nonuniform magnetic flux tubes with a finite curvature radius. The main aspect of our study is the influence of the curvature radius and magnetic field convergence on MHD wave propagations along a magnetic tube. The results obtained are corresponding to the par-

ticular case of the meridional polarization of the wave pulses propagating along curved axisymmetric magnetic field lines.

We obtained that a finite curvature radius of magnetic field lines brings about the interaction between transversal and field-aligned compressible perturbations. This interaction is more pronounced for larger plasma β parameters. The amplitude of the induced field-aligned velocity perturbation is proportional to the background plasma β parameter β_0, as well as to the ratio of the displacement of the magnetic field line δr and the curvature radius R, $\delta V_{\parallel} \sim 2\beta_0 V_a \delta r/R$. The magnetic field curvature affects also the dispersion of Alfvén waves which is dependent on the parameter $\beta_0/(kR)^2$, where k is the wave number.

The length scale of Alfvén perturbations propagating along a narrowing magnetic tube increases proportionally to the magnetic field strength. The amplitudes of velocity and magnetic field perturbations do not change much while the wave does not arrive at the reflection zone. This leads to a strong enhancement of the electric field amplitude during the wave propagation in the direction of the magnetic pressure gradient.

The reflection stage starts as soon as the length scale of the wave front becomes of the order of the distance from the boundary. The wave is reflecting rather from a very narrow "hole" of the magnetic tube than from the conducting boundary in cases of sufficient large wave length scales as well as large ratios of $S_{\max}/S_{\min}$, where $S_{\max}$ and $S_{\min}$ are the maximal and minimal cross sections of the magnetic tube. In such cases, the wave energy flux to the conducting surface at $r = r_{\min}$ is rather small, and thus the dissipation of the wave perturbations is very weak irrespective of a finite conductivity of the boundary. The wave length scale is a crucial parameter for the wave propagation along a strongly narrowing magnetic flux tube. As mentioned above, the wave length scale δ is increasing proportionally to the magnetic field strength in the course of the wave propagation $\delta \sim \delta_0 B(r)/B_0$. Reflection takes place when δ is of order of r, and thus the reflection zone can be estimated from the condition $\delta_0 B(r')/B_0 \sim r'$. For a dipole magnetic field, $B(r')/B_0 \sim (r_{\max}/r)^3$, and the last condition yields the estimation $r' \sim r_{\max}(\delta_0/r_{\max})^{1/4}$. A conducting boundary has a minor influence on the wave reflection if it has a sufficiently small size $r_{\min}$ with respect to r': $r_{\min}/(r_{\max} \ll (\delta_0/r_{\max})^{1/4}$. This is the case which is illustrated in our results of calculations.

Our results can be applied to conditions of the Earth's magnetosphere where the perturbations of the magnetic field and velocity can be generated near the magnetopause and also in the magnetotail. In particular, the Alfvén pulses can be produced by bursty reconnection of magnetic fields occurring at the dayside magnetopause in cases of a southward interplanetary magnetic field. These magnetic reconnection pulses are associated with so-called "flux transfer events" (FTE) which can be seen in observations.[15,16] The pulses can propagate along dipolelike magnetic flux tubes towards the ionosphere which has a finite conductivity. In this case, the ratio $r_{\max}/r_{\min}$ is about 10. Another possible application is that for Alfvén oscillations in coronal loops. In principle, our analysis can be considered to be complementary to the results of paper[17] where the model of a straight magnetic flux tube is considered, and thus the effects of a finite curvature radius as well as of convergence of the magnetic field lines are not studied. In the model,[17] the wave damping is indicated to be less for the longer periods. Our results are also favor of this tendency: In a narrowing magnetic tube, the dissipation is weaker for larger wave periods.

ACKNOWLEDGMENTS

The authors thank H. O. Rucker for fruitful discussions.

This work was supported by the INTAS-ESA projects (Project Nos. 99-01277 and YSF 2002-97), by Grants (Grant Nos. 04-05-64088, 04-05-64935, 03-05-20014_BNTS_a, and 03-05-20012_BNTS_a) from the Russian Foundation of Basic Research, by Grant (Grant No. 2.15.2) from the Program DPhS-16 of the Department of Physical Sciences RAS, by grants (Grant Nos. E02-8.0-22 and A03-2.13-469) from the Russian Ministry of Higher Education, and by project No. 1.2/04 from "Österreichischer Austauschdienst." It is also supported by the Austrian "Fonds zur Förderung der wissenschaftlichen Forschung" under Project Nos. P13804-TPH, P14744-TPH, and P17100-N08. We acknowledge support by the Austrian Academy of Sciences, "Verwaltungstelle für Auslandsbeziehungen," and the Russian Academy of Sciences.

APPENDIX: FROZEN-IN MATERIAL COORDINATES

In this section, we define frozen-in material coordinates which are very important for our. We introduce two coordinates as Euler potentials ϕ, ψ, which are determined by the equation

$$\mathbf{B} = \nabla \phi \times \nabla \psi. \tag{A1}$$

These potentials are constant along a magnetic field line and satisfy the equations

$$\mathbf{B} \cdot \nabla \phi = 0, \quad \mathbf{B} \cdot \nabla \psi = 0. \tag{A2}$$

Using these equations we can determine the potentials for all magnetic field lines. Near a planet, which is considered to be the source of magnetic field, these potentials ϕ and ψ can be identified with the magnetic latitude and longitude, respectively.

For each magnetic field line characterized by two constant parameters ϕ and ψ, we define a function $\alpha(s, \phi, \psi)$ depending on the distance s along the magnetic field line as follows:

$$\alpha = \int_0^s \rho/B ds'. \tag{A3}$$

For each magnetic field line, we imply the origin for α where it is equal to zero. The gradient of α along a magnetic field line is determined by the following equation:

$$\mathbf{B} \cdot \nabla \alpha = \rho. \tag{A4}$$

Finally, we have three variables α, ϕ, and ψ which can be used as independent coordinates. Now we have to prove that these quantities are material coordinates.

For this purpose, we consider Eqs. (A2) and (A4) as a linear algebraic system with respect to the three unknown quantities B_x, B_y, and B_z. The solution of this algebraic system is

$$B_x = \frac{\rho}{J}\frac{D(\phi,\psi)}{D(y,z)}, \quad B_y = \frac{\rho}{J}\frac{D(\phi,\psi)}{D(z,x)}, \quad B_z = \frac{\rho}{J}\frac{D(\phi,\psi)}{D(x,y)}, \tag{A5}$$

and J is defined as

$$J = \frac{D(\alpha,\phi,\psi)}{D(x,y,z)}. \tag{A6}$$

Here $D(\cdot)/D(\cdot)$ is a standard notation for Jacobians defined as determinants of matrices of partial derivatives, i.e.,

$$D(f_1, f_2, \ldots, f_n)/D(\xi_1, \xi_2, \ldots, \xi_n) = |A|,$$

$$A_{i,j} = \partial f_i/\partial \xi_j, \quad i = 1,2,\ldots,n, \quad j = 1,2,\ldots,n.$$

In a vector form, Eq. (A5) can be written as follows:

$$\mathbf{B} = \frac{\rho}{J}\boldsymbol{\nabla}\phi \times \boldsymbol{\nabla}\psi. \tag{A7}$$

Comparing Eqs. (A7) and (A1), we find the Jacobian to be $J=\rho$. Using the standard technique for Jacobian transformations, we find

$$B_x = \frac{\rho}{J}\frac{D(\phi,\psi)}{D(y,z)} = \frac{\rho}{J}\frac{D(x,\phi,\psi)}{D(x,y,z)} = \rho\frac{D(x,y,z)}{D(\alpha,\phi,\psi)}\frac{D(x,\phi,\psi)}{D(x,y,z)}$$
$$= \rho\frac{D(x,\phi,\psi)}{D(\alpha,\phi,\psi)} = \rho\frac{\partial x}{\partial \alpha}. \tag{A8}$$

Using analogous transformations for other components, we obtain

$$B_y = \rho\frac{\partial y}{\partial \alpha}, \quad B_z = \rho\frac{\partial z}{\partial \alpha}. \tag{A9}$$

The last three equations can also be written in a vector form

$$\mathbf{B} = \rho\frac{\partial \mathbf{r}}{\partial \alpha}. \tag{A10}$$

Furthermore, we use the induction equation for the frozen-in magnetic field, which can be written in the form

$$\frac{d}{dt}\left(\frac{\mathbf{B}}{\rho}\right) = \left(\frac{\mathbf{B}}{\rho}\cdot\boldsymbol{\nabla}\right)\mathbf{V}. \tag{A11}$$

Here $d(\cdot)/dt$ is the derivative along the trajectory of a fluid particle,

$$\frac{d(\cdot)}{dt} = \frac{\partial(\cdot)}{\partial t_{x,y,z}} + \mathbf{V}\cdot\boldsymbol{\nabla}(\cdot)$$
$$= \frac{\partial(\cdot)}{\partial t_{\alpha,\phi,\psi}} + \frac{d\alpha}{dt}\frac{\partial(\cdot)}{\partial\alpha} + \frac{d\phi}{dt}\frac{\partial(\cdot)}{\partial\phi} + \frac{d\psi}{dt}\frac{\partial(\cdot)}{\partial\psi}. \tag{A12}$$

Using Eqs. (A10), (A2), (A4), and (A11), and considering $\mathbf{B}$ and ρ to be functions of (α,ϕ,ψ,t), we get the equation

$$\frac{d}{dt}\left(\frac{\partial \mathbf{r}}{\partial \alpha}\right) = \frac{\partial \mathbf{V}}{\partial \alpha}. \tag{A13}$$

Taking into account the kinematic relation between velocity and position vector in the form of Eq. (A12), we get

$$\mathbf{V} = \frac{d\mathbf{r}}{dt} = \frac{d\mathbf{r}}{\partial t_{\alpha,\phi,\psi}} + \frac{d\alpha}{dt}\frac{\partial \mathbf{r}}{\partial\alpha} + \frac{d\phi}{dt}\frac{\partial \mathbf{r}}{\partial\phi} + \frac{d\psi}{dt}\frac{\partial \mathbf{r}}{\partial\psi}. \tag{A14}$$

Substituting Eq. (A14) into Eq. (A13) and using Eq. (A12), we finally obtain the equation

$$\frac{\partial^2\mathbf{r}}{\partial\alpha\partial t} + \frac{d\alpha}{dt}\frac{\partial}{\partial\alpha}\left(\frac{\partial\mathbf{r}}{\partial\alpha}\right) + \frac{d\phi}{dt}\frac{\partial}{\partial\phi}\left(\frac{\partial\mathbf{r}}{\partial\alpha}\right) + \frac{d\psi}{dt}\frac{\partial}{\partial\psi}\left(\frac{\partial\mathbf{r}}{\partial\alpha}\right)$$
$$= \frac{\partial^2\mathbf{r}}{\partial t\partial\alpha} + \frac{\partial}{\partial\alpha}\left(\frac{d\alpha}{dt}\frac{\partial\mathbf{r}}{\partial\alpha}\right) + \frac{\partial}{\partial\alpha}\left(\frac{d\phi}{dt}\frac{\partial\mathbf{r}}{\partial\phi}\right) + \frac{\partial}{\partial\alpha}\left(\frac{d\psi}{dt}\frac{\partial\mathbf{r}}{\partial\psi}\right). \tag{A15}$$

This equation can be simplified to

$$\frac{\partial\mathbf{r}}{\partial\alpha}\frac{\partial\dot{\alpha}}{\partial\alpha} + \frac{\partial\mathbf{r}}{\partial\phi}\frac{\partial\dot{\phi}}{\partial\alpha} + \frac{\partial\mathbf{r}}{\partial\psi}\frac{\partial\dot{\psi}}{\partial\alpha} = 0, \tag{A16}$$

where we use

$$\dot{\alpha} = \frac{d\alpha}{dt}, \quad \dot{\phi} = \frac{d\phi}{dt}, \quad \dot{\psi} = \frac{d\psi}{dt}.$$

We consider the vector equation (A16) as three scalar homogeneous algebraic equations versus the quantities $\partial(\dot{\alpha})/\partial\alpha$, $\partial(\dot{\phi})/\partial\alpha$, and $\partial(\dot{\psi})/\partial\alpha$.

The determinant of this system is the Jacobian J that is not equal to zero (see above, where $J=\rho$). For a nonzero determinant, this system has only the trivial solution,

$$\frac{\partial\dot{\alpha}}{\partial\alpha} = 0, \quad \frac{\partial\dot{\phi}}{\partial\alpha} = 0, \quad \frac{\partial\dot{\psi}}{\partial\alpha} = 0. \tag{A17}$$

According to our definition, for each magnetic field line, there exists a point where α is equal to zero. This condition and Eq. (A17) yield that $\dot{\alpha}=0$ everywhere.

The Euler potentials can be expressed through the latitude and longitude of a magnetic field line at the planet surface, where $\dot{\phi}=0$ and $\dot{\psi}=0$. These boundary conditions for Euler potentials together with Eq. (A17) lead to equations $\dot{\phi}=0$ and $\dot{\psi}=0$ everywhere. Thus the proved statement is

$$\frac{d\alpha}{dt} = 0, \quad \frac{d\phi}{dt} = 0, \quad \frac{\partial\psi}{dt} = 0. \tag{A18}$$

Therefore, the introduced independent variables α, ϕ, and ψ are material coordinates, and they conserve their values along trajectories of fluid particles.

From Eqs. (A14) and (A18) we obtain the simple relation between velocity and position vector,

$$\mathbf{V} = \frac{\partial\mathbf{r}}{\partial t_{\alpha,\phi,\psi}}. \tag{A19}$$

Using Eqs. (A2), (A4), and (A18), the dimensionless momentum equation can be written as follows:

$$\frac{d\mathbf{V}}{dt} + \frac{1}{\rho}\nabla\Pi - \frac{1}{\rho}(\mathbf{B}\cdot\nabla)\mathbf{B}$$
$$= \frac{\partial\mathbf{V}}{\partial t} + \frac{1}{\rho}\nabla\Pi - \frac{1}{\rho}\frac{\partial\mathbf{B}}{\partial\alpha}(\mathbf{B}\cdot\nabla\alpha) - \frac{1}{\rho}\frac{\partial\mathbf{B}}{\partial\phi}(\mathbf{B}\cdot\nabla\phi)$$
$$- \frac{1}{\rho}\frac{\partial\mathbf{B}}{\partial\psi}(\mathbf{B}\cdot\nabla\psi) = \frac{\partial\mathbf{V}}{\partial t} + \frac{1}{\rho}\nabla\Pi - \frac{\partial\mathbf{B}}{\partial\alpha} = 0. \quad \text{(A20)}$$

Using Eqs. (A2), (A4), and (A18), we transform the induction equation (A11) as well,

$$\frac{d}{dt}\left(\frac{\mathbf{B}}{\rho}\right) - \left(\frac{\mathbf{B}}{\rho}\cdot\nabla\right)\mathbf{V} = \frac{\partial}{\partial t}\left(\frac{\mathbf{B}}{\rho}\right) - \frac{\partial\mathbf{V}}{\partial\alpha} = 0. \quad \text{(A21)}$$

The MHD system of equations is closed by the adiabatic equation

$$\frac{d}{dt}(P/\rho^{\gamma}) = \frac{\partial}{\partial t}(P/\rho^{\gamma}) = 0. \quad \text{(A22)}$$

In principle, frozen-in coordinates can be introduced in different ways. The first application of frozen-in coordinates to space plasmas was proposed in Ref. 18.

[1] R. J. Defouw, Astrophys. J. **209**, 266 (1976).
[2] H. C. Spruit, Astron. Astrophys. **98**, 155 (1981).
[3] I. C. Rae and B. Roberts, Astrophys. J. **256**, 761 (1982).
[4] A. Ferriz-Mas, Phys. Fluids **31**, 2583 (1988).
[5] G. H. Fisher, Y. Fan, D. W. Longcope, M. G. Linton, and W. P. Abbett, Phys. Plasmas **7**, 2173 (2000).
[6] V. M. Nakariakov and L. Ofman, Astron. Astrophys. **372**, L53 (2001).
[7] D. J. Southwood and M. A. Saunders, Planet. Space Sci. **33**, 127 (1985).
[8] A. D. M. Walker, J. Geophys. Res. **92**, 10039 (1987).
[9] D. Y. Klimushkin, Ann. Geophys. **16**, 303 (1998).
[10] N. V. Erkaev, V. S. Semenov, V. A. Shaidurov, D. Langmayr, H. K. Biernat, and H. O. Rucker, Int. J. Geomagn. Aeron. **3**, 67 (2002).
[11] N. V. Erkaev, V. A. Shaidurov, V. S. Semenov, and H. K. Biernat, Nonlinear Processes Geophys. **9**, 163 (2002).
[12] A. I. Akhiezer, I. A. Akhiezer, R. V. Polovin, A. G. Sitenko, and K. N. Stepanov, *Plasma Electrodynamics* (Pergamon, Oxford, 1975).
[13] P. M. Edwin and B. Roberts, Sol. Phys. **88**, 179 (1983).
[14] C. E. McIlwain, J. Geophys. Res. **66**, 3681 (1961).
[15] J. Berchem and C. T. Russell, J. Geophys. Res. **89**, 6689 (1984).
[16] R. P. Rijnbeek, S. W. H. Cowley, D. J. Southwood, and C. T. Russell, J. Geophys. Res. **89**, 786 (1984).
[17] B. De Pontieu, P. C. H. Martens, and H. S. Hudson, Astrophys. J. **558**, 859 (2001).
[18] M. I. Pudovkin and V. S. Semenov, Ann. Geophys. **33**, 429 (1977).